JOURNAL OF EXPERIMENTAL AND THEORETICAL PHYSICS, 2024, Vol. 165, No. 4, pp. 474–488

ATOMS, MOLECULES, OPTICS

ATOMISTIC ANALYSIS OF RECOMBINATIVE DESORPTION OF HYDROGEN FROM TUNGSTEN SURFACE

© 2024 N. N. Degtyarenko*, K. S. Grishakov**, A. A. Pisarev, Yu. M. Gasparyan

National Research Nuclear University MEPHI,
115409, Moscow, Russia

**e-mail: nndegtyarenko@mephi.ru*
***e-mail: ksgrishakov@mephi.ru*

Received September 06, 2023
Revised December 08, 2023
Accepted December 08, 2023

Abstract. Within the density functional theory method, an analysis of the process of recombinative desorption of hydrogen atoms located on the surface and in the near-surface layers of tungsten W(100) is conducted. A mechanism for the growth of clusters of adsorbed hydrogen atoms on the tungsten surface is proposed. The calculation of activation energies for desorption processes for various configurations of adsorbed hydrogen atoms is performed. The dependence of the recombinative desorption activation energy on the local environment is shown. The lowest activation energy for recombinative desorption $\varepsilon_{des} \approx 0.9–1.0$ eV is achieved for a pair of H atoms, where one belongs to a cluster of hydrogen atoms adsorbed on the surface, and the other emerges from the subsurface layers of W(100).

Keywords: *tungsten, surface W(100), density functional theory, subsurface layers, hydrogen atoms, recombination desorption, clusters, activation energies*

DOI: 10.31857/S004445102404e023

1. INTRODUCTION

Thermonuclear fusion is considered to be a promising source of energy on Earth. An important issue for thermonuclear reactors is the selection of materials capable of withstanding abnormally high hydrogen plasma fluxes in the specific region called the divertor. Among the materials considered for plasma-facing components (PFC) of the divertor, tungsten was chosen due to its set of properties [1]. In particular, PFCs in the divertor region of the International Thermonuclear Experimental Reactor (ITER) experimental reactor under construction will be made of W [2]. Besides high heat fluxes, hydrogen isotopes also isotopes cause serious problems related to the degradation of structural properties and radiation hazard. For this reason, the capture of hydrogen ions in tungsten and the control of the hydrogen isotopes content have been subjects of intensive research for many years [3, 4]. The issues of hydrogen capture and release play an important role in hydrogen storage technologies as well [5].

One of tungsten's advantages is its very low hydrogen solubility, which should help to reduce problems with tritium accumulation. However, at high concentrations of radiation defects, the accumulation of hydrogen isotopes in tungsten increases significantly [6]. Low solubility and the significant influence of defects make it extremely difficult to experimentally determine even basic characteristics of hydrogen interaction with the tungsten lattice, such as the diffusion coefficient and binding energy with point defects [7]. Therefore, there is growing interest in *ab initio* calculations based on the density functional theory (DFT).

Elementary processes on the surface, due to the influence of multiple factors related to the surface structure and presence of impurities, are difficult to study experimentally. Detailed theoretical studies allow identifying the main mechanisms of processes occurring on the surface and can be used to interpret experimental data. For predicting hydrogen recombinative desorption processes from tungsten surfaces, a system of diffusion-kinetic balance equations is mainly used, with energy parameters often determined through DFT calculations [8, 9].

When studying hydrogen adsorption and desorption processes on tungsten surfaces, the structure of the smooth surface is a significant factor. Studies conducted within DFT showed that the surface W(110) is the most stable compared to W(100), W(111), and W(211) [10–15]. Therefore, most studies analyzing hydrogen behavior on the surface have been performed for W(100). However, structural materials are typically not texturized and are characterized by a variety of grain orientations. Therefore, it is of interest to conduct a detailed analysis of hydrogen adsorption and desorption processes, including on the W(100) surface.

At temperatures around room temperature and above, the smooth surface W(100) has $p(1\times1)$ periodicity [16, 17], while at temperatures below a certain critical point $T_c \sim 250$ K, the smooth surface W(100) reconstructs into a more energetically favorable one with $c(2\times2)$-structure [17]. DFT calculations confirm this surface reconstruction [18–22]. The reconstruction mainly affects the top surface layer of tungsten atoms, with the distance from which the degree of reconstruction decreases [18, 19]. The interlayer distance between the top surface layer and the first subsurface layer, calculated in DFT, is 1.48 Å, which agrees well with experimental results [18, 23]

Experiments show that hydrogen is adsorbed on W(100) in atomic form [24] in a position between two tungsten atoms of the upper surface layer, which is referred to in literature as "bridge" [25]. Experiments give adsorption energy values of 0.7 eV and 0.82 eV [26–28].

Theoretical studies within DFT framework agree with experimental results, providing a more detailed picture of adsorption. DFT calculations show that for the unreconstructed W(100) surface, adsorption at the "bridge" position is most favorable, with the adsorption energy of $E_{ads} \approx -1.16$ eV (including zero-point energy) [3]. The adsorbed hydrogen atom causes some surface reconstruction. For a smooth unreconstructed surface, the distance W–W is 3.17 Å, and upon hydrogen adsorption, tungsten atoms relax towards H, approaching to a distance of 2.61 Å [3]. In the case of reconstructed W(100) surface, DFT calculations show that there are two different positions of the adsorbed hydrogen atom corresponding to an energy minimum [3, 22, 29]. These positions are referred to in literature as "short bridge" and "long bridge" and for a smooth surface are characterized by W–W distances of 2.82 Å and 3.57 Å, respectively [3]. Hydrogen adsorption in the "short bridge" position is more energetically favorable (including the zero-point energy $E_{ads} \approx -0.88 \div -0.91$ eV), compared to adsorption in the "long bridge" position ($E_{ads} \approx -0.46 \div -0.47$ eV) [3, 22, 29]. Hydrogen adsorption in "short bridge" and "long bridge" positions causes some surface reconstruction W(100): the distance W–W for tungsten atoms nearest to the adsorbed hydrogen decreases to 2.64 Å for the "short bridge" position and to 3.21 Å for the "long bridge" position [3]. The calculations also yielded geometric parameters characterizing the adsorbed hydrogen atom on the surface W(100): the bond length W–H $\approx$ 1.91–1.94 Å, the angle W–H–W $\approx$ 87.1–87.8°, and the distance between H and the plane containing the top surface layer of W atoms 1.36–1.38 Å [22, 29, 30].

Since the adsorption of a hydrogen atom, regardless of the presence or absence of reconstruction of the smooth surface, W(100) leads to changes in W–W interatomic distances, the surface structure may depend on the degree of hydrogen coverage. In work [31], theoretical calculations showed that for a smooth surface, W(100) reconstruction disappears at a surface coverage of $\theta \geq 1.5$, and the energy of hydrogen adsorption on the W(100) surface decreases almost linearly with increasing the surface coverage, reaching a minimum value at a coverage of $\theta = 2$. Further increase in coverage leads to an increase in the adsorption energy. Experimental studies conducted in work [32] also demonstrate the dependence of surface reconstruction on temperature and hydrogen coverage.

Active research was conducted on diffusion of adsorbed hydrogen along the W(100) surface. For the reconstructed surface, DFT calculations give the following activation energy values: 0.35–0.43 eV for transition between two "short bridge" positions; 0.44 eV for transition between two "long bridge" positions; 0.53–0.65 eV for transition between "short bridge" and "long bridge", and 0.11–0.21 eV for the reverse process [3,29]. The lower value of the energy barrier during transition between "long bridge"–"short bridge" positions is due to the fact that the "long bridge" position is metastable. In the established state during diffusion of an

adsorbed hydrogen atom along the W(100) surface, transitions between "short bridge" positions should be expected with a higher probability. In work [29], the pre-exponential factor for diffusion of adsorbed hydrogen between two "short bridge" positions was also theoretically determined, which was $0.5 \cdot 10^{-2}$ cm^2/s. Similar experimental studies showed that for H diffusion on the surface W(100) at a surface coverage of $\theta = 0.08$ and in the temperature range of 220–300 K, the pre-exponential factor and the activation energy are $1.2 \cdot 10^{-2}$ cm^2/s and 0.47 eV, respectively [33], which agrees quite well with theoretical calculations.

The next issue that has been studied in detail in the literature is the migration of hydrogen atoms from the tungsten bulk to the surface and the corresponding reverse process. The main result of most works in this direction is the energy instability of a single hydrogen atom in the subsurface layers of W(100). The location of hydrogen on the surface is significantly more energetically favorable (by approximately 2 eV) [3, 22, 29, 30, 34]. The DFT-calculated activation energy for the migration process of a hydrogen atom from the surface state to the bulk is about 2 eV [3, 22, 29, 30, 34]; such a barrier is overcome with a finite probability only at temperatures of about 800 K and higher [30]. The reverse process of hydrogen atom transition from the tungsten bulk to the surface W(100) occurs spontaneously from the first subsurface layer (the activation barrier is no higher than 0.01 eV), while the transition between deeper subsurface layers is characterized by very small barriers, 0.1–0.27 eV [3, 22, 29, 30, 34]. Model calculations in [22] show that hydrogen atoms repel each other in subsurface layers, therefore hydrogen cluster formation in the subsurface region does not occur without presence of defects in the tungsten structure. Therefore, it should be expected that the process of hydrogen release from the bulk onto the surface will occur spontaneously at room temperatures.

Along with hydrogen adsorption on the tungsten surface, the study of the desorption process is important. Experimental works show that at a low hydrogen surface coverage of W(100) the desorption activation energy is about 1.65 eV [28]. An increase in the surface coverage to $\theta = 0.46$ leads to a significant decrease in the desorption activation energy to about 0.92 eV [28]. DFT calculations qualitatively confirmed the experimental result about the decrease in the desorption energy with increasing surface coverage of W(100) [35–37]: the desorption activation energy at a low coverage is 1.5 eV, and at full coverage equals 1.0 eV [35, 37]. Based on molecular dynamics calculations with three-body interaction potential [8], it is shown that at high values of θ there exists a regime when large hydrogen clusters form on the tungsten surface and a sharp increase in desorption intensity is possible, which are also observed experimentally [38]. In work [8], it is noted that hydrogen desorption from tungsten surface may not always be the second-order process, and the need for better estimation of W–H and H–H the interatomic interactions on W surface is emphasized, for example, within the DFT method.

Despite detailed studies of hydrogen adsorption and desorption processes on tungsten surface, several questions remain open. In particular, there is the question about the optimal value of d(H–H) for minimizing the activation energy for recombinative desorption. The question of surface cluster formation from adsorbed atoms in the presence of dissociative chemisorption phenomenon is also not obvious, since most works consider ultimate cases of uniform coverage. Hydrogen recombination and desorption processes on tungsten surface in most works are assumed as separate processes, but details of this process are not considered. The probability of recombinative desorption process depends on a large number of integral and local conditions: in particular, on the flux of interstitial hydrogen atoms to the surface from the bulk, on the local surface state and temperature, on the local environment of the atom pair participating in the recombinative desorption process, rather than on the average surface coverage.

The aim of this work is to refine, within the framework of density functional theory, the atomistic picture of hydrogen desorption from the W(100) surface, specifically, calculating the possibility of formation and growth of hydrogen clusters on the surface, comparing desorption channels, analyzing the influence of W–W, W–H, and H–H configurations on activation barriers for recombinative desorption, considering the interaction of adsorbed hydrogen atoms and those diffusing from subsurface layers.

2. CALCULATION METHOD

Numerical calculations were performed using the density functional theory method with the plane wave basis in Quantum Espresso program [39, 40]. The PBEsol exchange-correlation functional was used, along with the norm-conserving pseudopotential, with the cutoff energy of 650 eV. In the reciprocal space, a grid was used with the distance between points not exceeding 0.05 $Å^{-1}$ along each coordinate. When modeling the surface, surface supercells were created containing 4×4 elementary tungsten cells. Along the Z axis, seven atomic layers were set, corresponding to 112 W atoms (in some variants, nine atomic layers were set, corresponding to 144 W atoms). A vacuum region of approximately 15 Å thick is situated over the upper layer of W atoms. During geometric optimization of the surface model, the coordinates of tungsten atoms in the three (or five) lower layers were considered fixed. Energy convergence conditions were $\Delta E \leqslant 2 \cdot 10^{-5}$ eV/atom, force convergence conditions were $F \leqslant 0.05$ eV/Å. After cell optimization, hydrogen atoms or molecules were introduced into the system, and structure re-optimization was performed with hydrogen participation. The search for optimal energy barriers during system transition from one configuration to another was carried out using the NEB (nudged elastic band) method. In this work, the energy reference level is taken as the total energy of the optimized system E_0 with adsorbed hydrogen atoms – the state with the lowest energy. In this case, for example, the activation energy for recombinative desorption is determined as $\varepsilon_{des} = E_1 - E_0$, where energy E_1 is the total energy of the optimized system after the desorption product leaves the system surface.

3. RESULTS

3.1. Energy characteristics of hydrogen behavior near W(100) surface

The behavior of the system's total energy is considered for different positions of the hydrogen molecule and atom near the smooth W(100) surface (see Fig. 1). Initial positions of the hydrogen atom and the H_2 molecule were set, and then the procedure of geometric optimization followed by calculations of activation energies were carried out, after which the total energy was calculated.

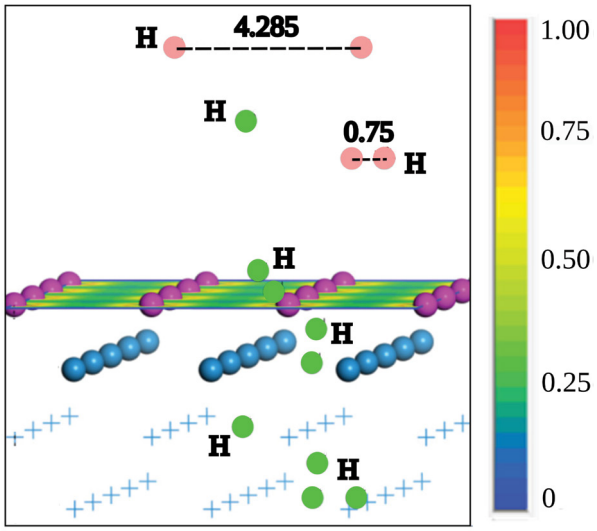

Fig. 1. Different initial positions of a single H atom (green spheres) and H atom pairs (pink spheres) with varying interatomic distances. A color map of the electron density distribution on the surface is presented in the range [0–1] electron/$Å^3$. The W atoms of the top surface layer here and further are shown as purple spheres, W atoms of the second layer and deeper layers under the surface are depicted as blue spheres and blue crosses, respectively

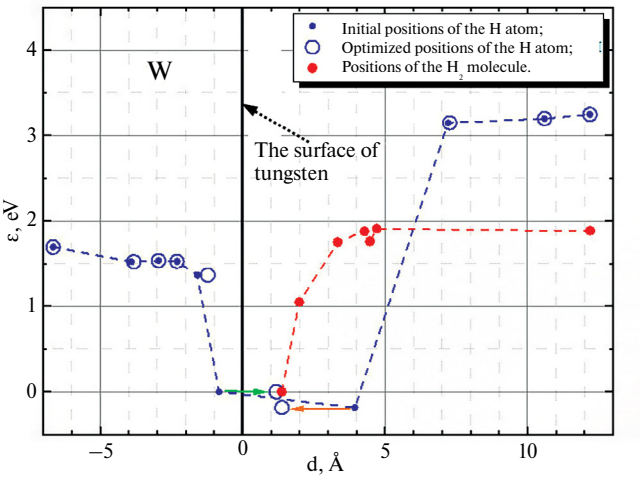

Fig. 2. Dependence of the system energy on hydrogen position relative to W(100) surface. The distance to the surface is plotted on the x-axis. The vertical solid black line marks the level of the W surface. The green arrow indicates the transition of a hydrogen atom from the bulk to the adsorbed state. The orange arrow shows the transition from the state above the surface to the adsorbed state. The total energy of the optimized configuration with hydrogen atoms adsorbed on the surface is taken as the energy reference level

Fig. 2 shows the dependence of the system energy on the position of the atom and hydrogen molecule. Initial positions (non-optimized) are shown in Fig. 2 as dots, while positions obtained through geometric optimization of the system are shown as empty circles. Below the W(100) surface, stable positions

for H atoms are in in tetrapores, located deeper than the second layer of tungsten atoms (distances from the surface more than 1.5 Å). Hydrogen atoms located between the first and second layers of tungsten atoms (distances less than 1 Å from the surface) spontaneously (without activation) emerge onto the surface (shown by green arrow in Fig. 2). Note that in the W bulk, the equilibrium tetrahedral positions of the interstitial H atom are separated by an energy barrier of $\varepsilon_{dif} \approx 0.1$–$0.27$ eV [3, 22, 29, 30, 34]. Thus, without any defects in the tungsten structure, hydrogen atoms need to overcome a relatively small energy barrier of about ε_{dif} to emerge from deep subsurface layers onto the surface.

A hydrogen atom initially placed above the surface at a distance less than approximately 4 Å transits to an adsorbed state in the "bridge" position with a distance to the surface of about 1.3 Å (shown by orange arrow in Fig. 2). After adsorption of an atom on the surface, the distance between two other tungsten atoms closest to the adsorbed hydrogen atom decreases from 3.16 Å to approximately 2.9 Å. This position for an isolated adsorbed atom is the most energetically favorable and remains so as the surface coverage increases up to maximum. The minimum optimized distance between two hydrogen atoms is $d_{min} \approx 2.3$ Å.

Thus, the region from which the individual hydrogen atoms are captured into the adsorbed state on the surface W(100) from both the bulk and vacuum side has a size of about 5–6 Å.

The chemisorption region for hydrogen molecules is slightly smaller, approximately 3 Å, and extends from the metal surface only into vacuum. The decomposition of the hydrogen molecule begins at a distance of about 3 Å from the tungsten surface. The dissociation occurs without activation. After molecular dissociation, the atoms are positioned above the surface in adjacent "bridge" positions at a distance of about 1.3 Å from the surface. The heat of chemisorption of two atoms is about $\varepsilon_{hem} \sim 2$ eV.

Absorption of hydrogen atoms from the chemisorption site occurs endothermically with an energy of about 1.5–1.6 eV (Fig. 2). As the hydrogen atom moves deeper into the metal, the system energy in equilibrium atomic positions gradually increases and already in the second interlayer becomes close to values characteristic of greater depths. It should be emphasized that in calculations of all configurations, the tungsten atoms of the upper four layers were mobile and their positions were also optimized.

A comparison was made of the total energies of two configurations with different positions of adsorbed atoms at a coverage of $\theta = 1$ (Fig. 3). In all further figures in the article, the adsorbed hydrogen atoms are depicted as green balls. In the first configuration, hydrogen atoms are located over the first layer in the bridge position, in the second – above the centers of faces (hollow position). In these two configurations, the distance between the nearest adsorbed atoms is the same and equals $d(\mathrm{H}-\mathrm{H}) \approx 3.16$ Å. The energy gain

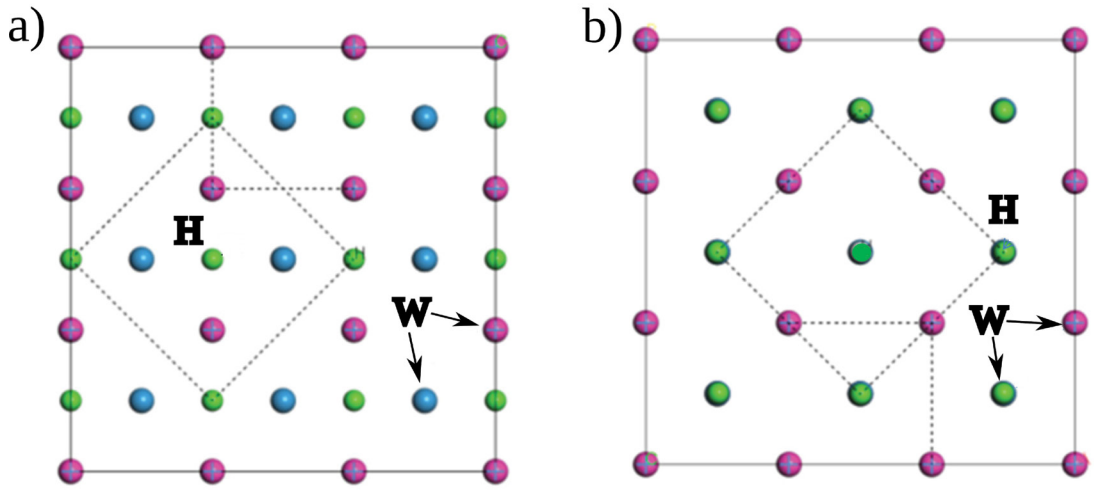

Fig. 3. Distribution of adsorbed hydrogen atoms on the surface W(100) at the coverage of $\theta = 1$. Interatomic distance $d(\mathrm{H}-\mathrm{H}) \approx 3.16$ Å: a – hydrogen atoms are located above the middle of the edges of the upper faces of W elementary cells (bridge position); b – hydrogen atoms are located above the W atoms of the second layer, covering them in the presented top view (hollow position)

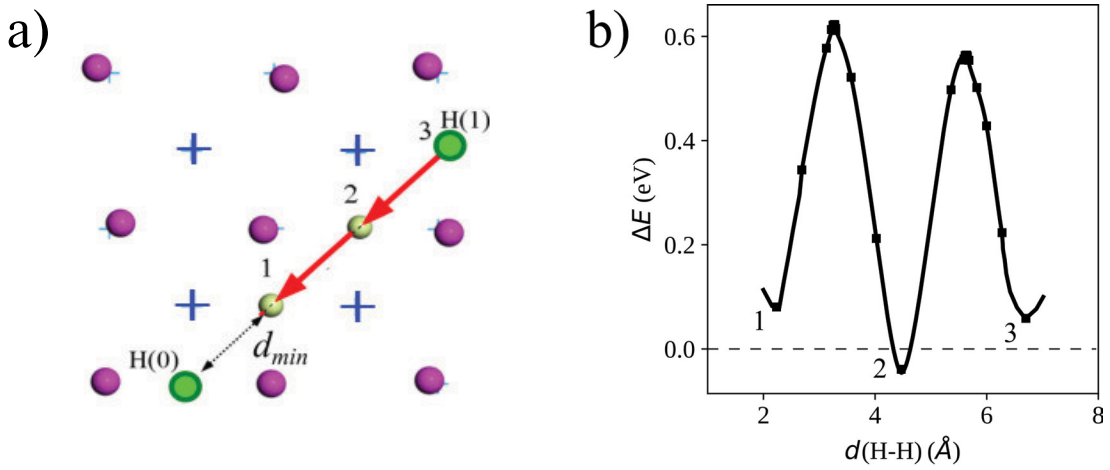

Fig. 4. a – Scheme of sequential approach of the adsorbed atom H(1) in position 3 to atom H(0) in position 1; b – change in system energy along the approach trajectory

for the first configuration is $\Delta\varepsilon \approx -0.32$ eV/(H atom), which shows the preference for distribution in the "bridge" positions (Fig. 3a). The "bridge" type configuration allows for an increase in the coverage up to $\theta = 2$ if H atom appears in the adjacent edge with $d(\text{H}-\text{H}) \approx 2.3$ Å, which is important for consideration of dense clusters of hydrogen atoms on the surface.

From the presented results and literature review, it is evident that there is a sufficiently strong interaction between adsorbed hydrogen atoms and tungsten atoms, which leads to the phenomenon of chemical adsorption – the decomposition of molecular hydrogen into atoms. DFT calculations show that near the tungsten surface, there is a change in the electronic state of not only the molecule but also the adsorbed hydrogen atom. The Hirshfeld charge for the adsorbed hydrogen atom above the metal surface is negative and equals $Z_H(\text{H}) \sim -0.2$ for the isolated state. Furthermore, at least two nearest neighbour tungsten atoms move closer to each other, compensating for the partial transfer of electron density to the hydrogen atom. During surface diffusion of an isolated hydrogen atom, there is also a movement of local changes in the electron density of the nearest tungsten atoms.

3.2. Interaction of adsorbed hydrogen atoms on W(100) surface

Let's consider the process of the two hydrogen atoms approaching each other when adsorbed on a smooth tungsten surface, which is illustrated in Fig. 4a. As noted above, there should be not only interaction between two H atoms but also local perturbations involving tungsten atoms. Fig. 4a shows two atoms, H(0) and H(1). The first of them remains in the same position, while the second successively occupies positions 3, 2, and 1. The system along the path is optimized, and the energy barrier between these states is searched using the NEB technique. Fig. 4b shows the system energy changing as one H atom moves toward another from a distance of $d(\text{H}-\text{H}) \sim 3d_{min}$ to $d(\text{H}-\text{H}) \sim d_{min}$. The value of energy in the optimized system with maximally separated hydrogen atoms $d(\text{H}-\text{H}) \sim 4d_{min}$ is taken as the reference level. The energy minima at positions 1, 2, and 3 in Fig. correspond to the respective positions in Fig. 4a. The energy value at these minima differs insignificantly, $\Delta E \approx 0.1$ eV. The barrier during transition from one minimum to another is approximately 0.5–0.6 eV, which is somewhat higher than the activation energy for surface diffusion of an isolated H atom (0.22–0.43 eV [3, 29, 41, 42]). The Hirshfeld charge in optimized configurations 1, 2, 3 (Fig. 4a) is approximately the same. The process of local electron density perturbations when one of the H atoms approaches to another differs from the case of movement of an isolated H atom, which leads to some increase in energy barriers compared to the activation energy for diffusion of an isolated atom.

Thus, the convergence of two undividual adsorbed H atoms through surface diffusion is an

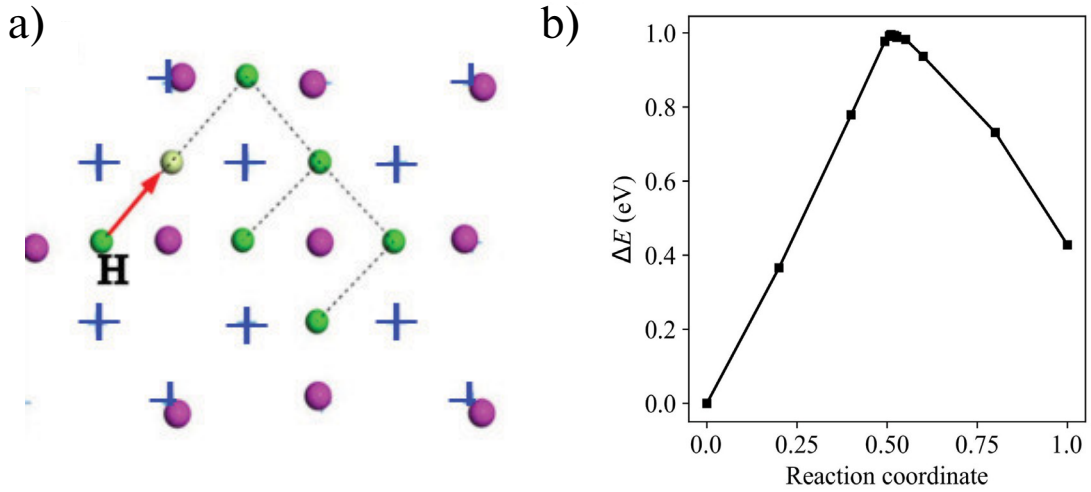

Fig. 5. a – Scheme of an individual adsorbed hydrogen atom approaching a cluster of 5 H atoms; b – change in system energy along the approach trajectory. The reaction coordinates are given in relative units from 0 in the initial psition to 1 in the final position.

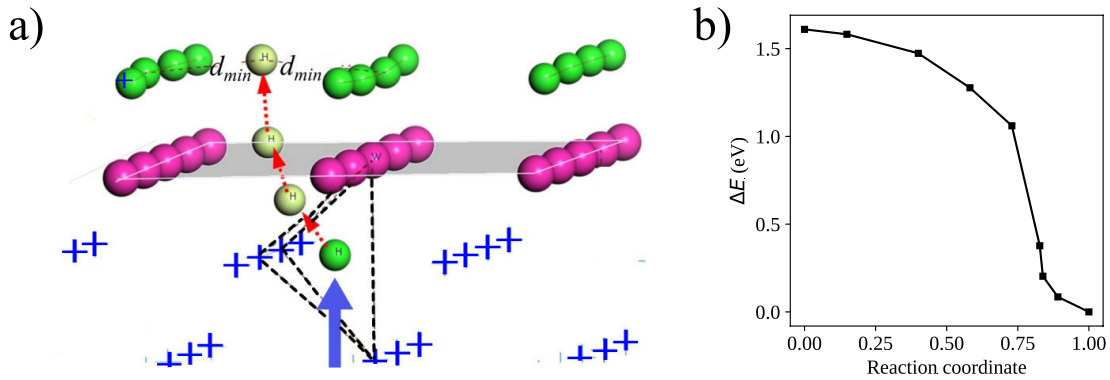

Fig. 6. a – Stages of interstitial hydrogen atom emergence from a subsurface tetrapore into the layer of adsorbed atoms with the iniform coverage θ = 1. The initial position of the H atom emerging from the bulk is shown by a bold blue arrow. All W atoms in the bulk are depicted by crosses. The W(100) surface is highlighted in gray; b – change in the system energy along the path shown in Fig. 6a, with the reference energy level corresponding to H atom in the adsorbed state

unlikely process due to a ruther high activation energy. Therefore, both recombinative desorption and the formation of a hydrogen atom dumbbell are unlikely under these conditions. With increasing temperature, the probability of overcoming energy barriers and recombination desorption increases.

Let's consider the possibility of hydrogen cluster growth through surface diffusion of a distant hydrogen atom. Here and further, we use the term "cluster" to denote accumulations of adsorbed atoms. Let's assume that there is a dense cluster of 5 H atoms on the tungsten surface with the interatomic distance d_{min}. A possible mechanism for the formation of such clusters is considered further. Let's examine the transition of a hydrogen atom, which is initially located at a distance of 4.5 Å from the cluster, into its composition, i.e., to a distance of d_{min} from the nearest cluster atom (see Fig. 5a). The calculation of the energy barrier for such a process (see Fig. 5b) gives a value of $\varepsilon_1 \approx 1$ eV. The reaction coordinates in Fig 5b (and similar figures) are given in relative units from 0 in the initial psition to 1 in the final position along the path calculated using the NEB method. The barrier for the reverse process (detachment from the cluster) is $\varepsilon_2 \approx 0.6$ eV. Meanwhile, the configuration with the H atom separated from the dense cluster has a lower energy. Such an interaction character has similarities with the process of hydrogen chemisorption on the surface. After dissociation, hydrogen atoms prefer to move apart to greater distances when free spaces are available on the surface. Thus, cluster growth through surface convergence with adsorbed hydrogen atoms is energetically unfavorable.

3.3. Interaction of hydrogen atoms adsorbed on W(100) surface with hydrogen atoms "surfacing" from the tungsten bulk

If cluster growth through diffusion along the surface is energetically unfavorable, then it is probably possible through diffusion of atoms dissolved in the bulk towards the surface. The latter option is interesting for many applications, for example, for analyzing desorption from metal into which hydrogen was introduced either from gas, plasma, ion irradiation, or through radioactive decay. This section examines the situation when an atom from the metal bulk approaches a surface densely covered with hydrogen.

Fig. 6 shows a uniform coverage with $\theta = 1$ (full coverage corresponds to $\theta = 2$) with the arrangement of adsorbed H atoms in optimized positions with the interatomic distance $d(\mathrm{H-H}) \approx 3.15$ Å and an interstitial hydrogen atom, which initially is located in the near-surface layer of tungsten in a tetrapore. Let's consider the transition of this atom from under the surface into the layer of adsorbed hydrogen atoms with interatomic distance d_{min}. Calculations show that the process of H atom transition from the first under-surface onto the surface is barrier-free. This means that after hydrogen atoms diffusing in the bulk, reach the first under-surface, they spontaneously emerge onto the surface with the activation energy $E_s = 0$ (see Fig. 6b). After reaching the surface, the atom occupies an energetically favorable position just like the other adsorbed atoms in the cluster. Due to this, the local coverage degree increases.

These results suggest that dense clusters with interatomic distance d_{min} can probably be created not through the convergence of adsorbed atoms along the surface, but through the process of local "surfacing" of interstitial H atoms that reach the under-surface of tungsten through diffusion.

3.4. Growth of two-dimensional clusters of adsorbed H atoms on atomically smooth surface

It can be assumed that after the "surfacing" of an H atom from the near-surface layers of tungsten under the center of a small dense cluster of hydrogen atoms, the atom can emerge into the first layer of adsorbed atoms, and the cluster can grow. Let's consider such a situation for the case of a small cluster of four hydrogen atoms with interatomic distance d_{min} (Fig. 7a). In such a cluster, all its atoms are peripheral. The optimized configuration of this state is stable, as the vibration frequency spectrum of the hydrogen subsystem in this state contains no imaginary frequencies.

Fig. 8 shows the sequence of events after a hydrogen atom "emerges" with a lateral displacement from the center of the cluster. In this case, there is an increase in the number of particles in the cluster. Fig. 8 shows that the emerged atom pushes one of the cluster atoms to its periphery, and takes its place.

That is the initial structure of a small cluster (Fig. 8a) becomes unstable when a hydrogen atom appears under this cluster due to nonactivated emergence from the underlying layers; and this leads to cluster growth and local coverage increase. Calculations show that there is no energy barrier for such restructurization, with a monotonic decrease in the total system energy.

Thus, when hydrogen atoms appear under the surface of a small cluster (with the number of atoms at least less than 6) or near the boundary of a large cluster (for example, due to diffusion from the metal bulk), these clusters may grow.

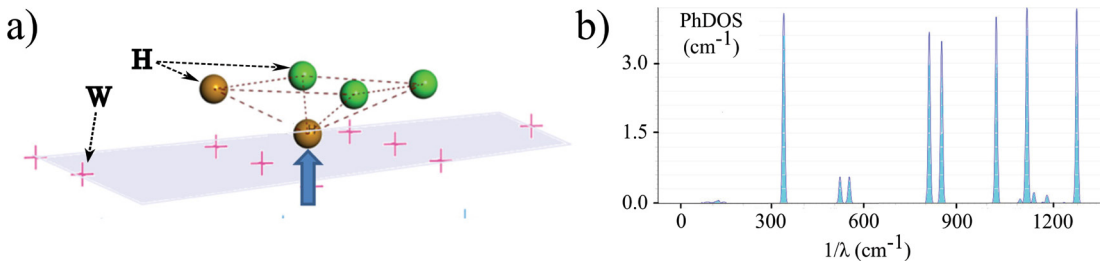

Fig. 7. a – Cluster of four adsorbed H atoms and a hydrogen atom "emerged" from the bulk under the cluster (highlighted by bold arrow); b – partial vibration spectrum of the hydrogen atoms system shown in Fig. 7a. The recombining pair of H atoms (here and in Fig. 8) is highlighted in brown

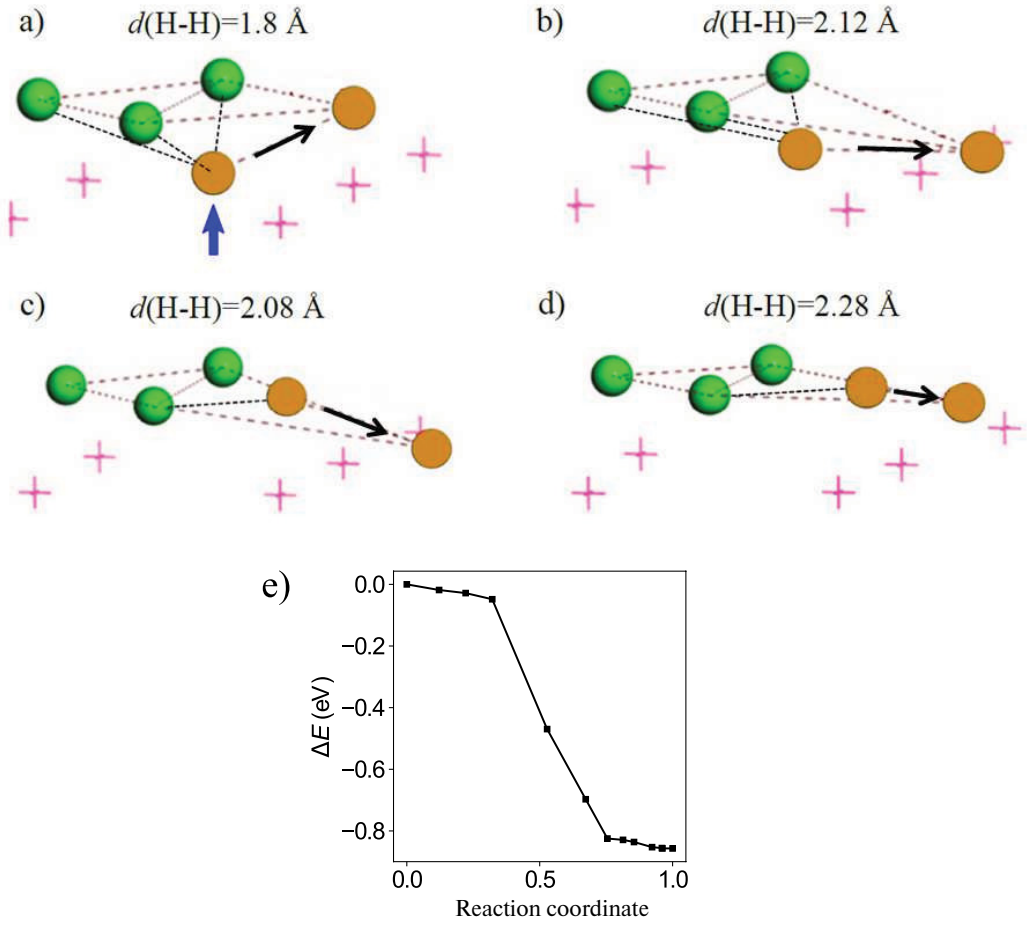

Fig. 8. a, b, c, d – Growth of a small cluster due to H atom emergence from the bulk (shown by blue arrow in Fig. 8a). Black arrow shows the direction of pushing one of the cluster atoms to its periphery; e – change in system energy during the movements shown in Fig. a, b, c, d (the energy of the initial system is taken as the reference level)

3.5. Oscillations of the system of adsorbed hydrogen atoms

Let's consider two hydrogen atoms adsorbed on the tungsten surface W(100) and located at a distance of $d(\mathrm{H-H}) = 6.7$ Å from each other. In this case, direct interaction between H atoms is practically excluded. Calculations of the vibrational spectra of such a system show that in the IR spectrum, the highest intensity is possessed by non-synchronous oscillations of hydrogen atoms with a frequency of 1160 cm^{-1} perpendicular to the surface. The remaining modes have low intensity and are mainly associated with hydrogen oscillations along the surface. In general, at low concentrations of adsorbed hydrogen atoms, when they are not clustered, their vibrations on the surface have modes characteristic of isolated adsorbed H atoms.

Let's investigate how the convergence of hydrogen atoms adsorbed on the tungsten surface affects their vibrational spectrum. Let's consider a simple system with four adsorbed hydrogen atoms forming the simplest linear cluster with interatomic distance d_{min} (Fig. 9a). In the IR spectrum of vibrations of such hydrogen cluster on the tungsten surface (Fig. 9b), 12 "main" modes can be distinguished in three frequency regions: $\nu \sim 490$ cm^{-1}, ~ 1060 cm^{-1}, and ~ 1260 cm^{-1}. Additionally, hydrogen atoms participate in the vibrational modes of surface tungsten atoms at frequencies less than approximately 200 cm^{-1}. At frequencies $\nu \approx 490$ cm^{-1} hydrogen atoms oscillate mainly along the surface in antiphase relative to each other. The mode with the frequency $\nu \approx 1063$ cm^{-1} corresponds to synchronous oscillations of two central hydrogen atoms perpendicular to the surface, and such oscillations can lead to synchronous

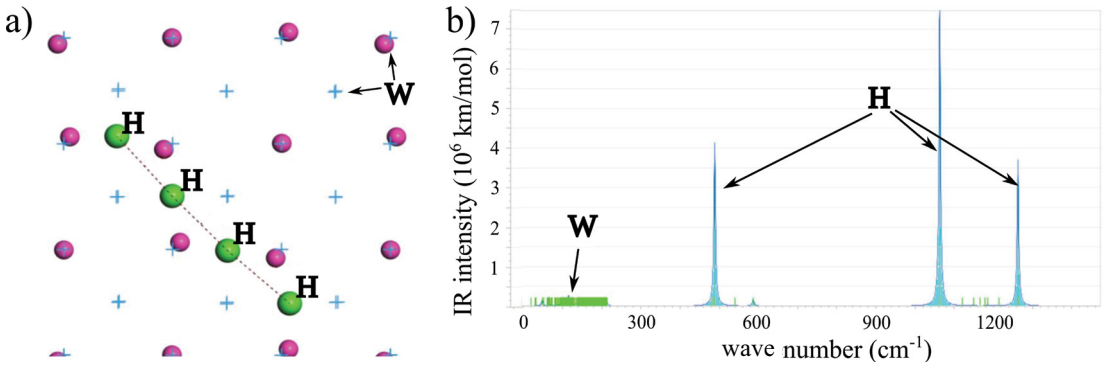

Fig. 9. a – Linear cluster of four adsorbed hydrogen atoms with interatomic distance of about d_{min}, top view, b – IR spectrum of a linear cluster of four adsorbed hydrogen atoms with interatomic distance d_{min} on the surface W(100), the intensity of spectral lines of some modes is close to zero

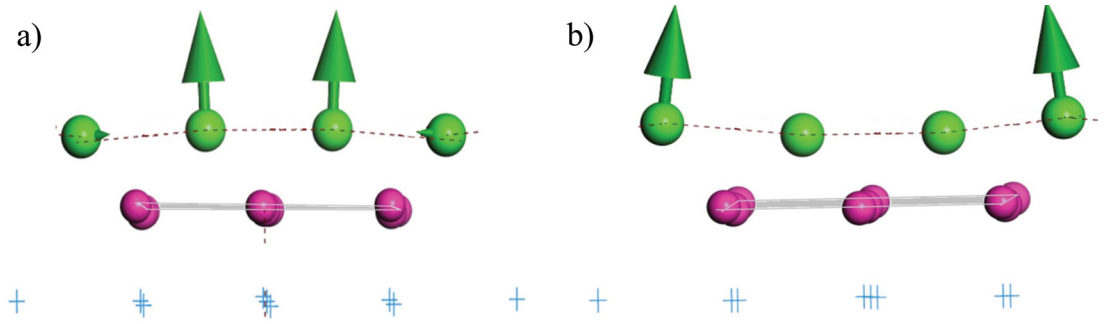

Fig. 10. a – Eigenvectors of synchronous displacements of two internal atoms of the linear cluster that take place perpendicular to the surface with frequency $\nu \approx 1063\ cm^{-1}$, b – eigenvectors of synchronous displacements of two side atoms of the linear cluster that take place perpendicular to the surface with frequency $\nu \approx 1263\ cm^{-1}$

release of H atoms from the surface with subsequent recombination (see Fig. 10a). The IR intensity of this mode is maximal. The mode with the maximum frequency $\nu \approx 1263\ cm^{-1}$ corresponds to in-phaseoscillations of two side atoms in the linear chain in the direction perpendicular to the surface (Fig. 10b).

A similar calculation was performed for a dense cluster of eight adsorbed H atoms with an interatomic distance of $d(H{-}H) = 2.3$ Å, having a nonlinear configuration. Overall, the vibration spectrum for the dense cluster is similar to the case of the linear cluster. The main difference is the increase in the total number of modes, as well as an increase in the frequency of high-frequency vibrations to values around $1300\ cm^{-1}$ ($\nu \approx 32$ GHz).

The presence of in-phase vibrations of two nearest hydrogen atoms, perpendicular to the surface, is likely a necessary precondition for desorption of a molecule H_2 from the cluster with a frequency of $\nu \approx 32$ GHz. The appearance of such vibration modes is due to the "close" arrangement of atoms in dense clusters with the local hydrogen coverage $\theta = 2$.

3.6. Desorption of two isolated atoms

Let's consider two closely located (at a distance of d_{min}) hydrogen atoms on the W(100) surface. Calculations show that the release of these atoms into vacuum with the formation of a molecule H_2 has a significantly lower activation energy of $\varepsilon_{des}(H_2) \approx 1.85$ eV compared to the activation energy for the release of two individual hydrogen atoms without molecule formation of $2\varepsilon_{des}(1H) \approx 6.44$ eV.

For recombinative desorption of a pair of hydrogen atoms at distances between them greater than a minimum, the trajectory of atom convergence is essential. Fig. 11 shows two possible recombination sequences of atoms located above opposite edges of the tungsten cell at a distance $d(H{-}H) \approx 3.3$ Å. Fig. 12 shows the change in the total system energy in these two cases depending on the distance between the atoms.

For the first trajectory (Fig. 11a), H atoms initially move predominantly upward without changing the interatomic distance and then come closer together. This is the most unfavorable trajectory. The total system energy along this trajectory passes

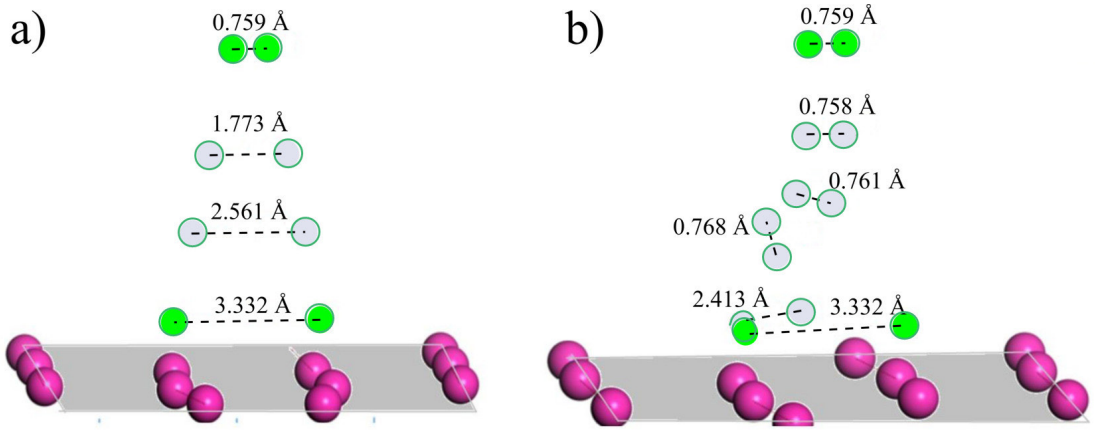

Fig. 11. Trajectories of two different desorption paths for hydrogen atoms initially located on the tungsten surface at a distance of d(H–H) ≈ 3.3 Å

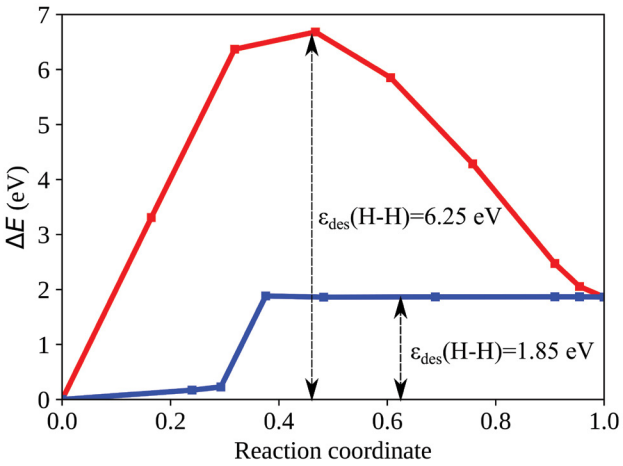

Fig. 12. Change in the total system energy during hydrogen atom desorption along two different trajectories. The red curve corresponds to the trajectory shown in Fig. 11a, and the blue line corresponds to the trajectory shown in Fig. 11 b

through a maximum corresponding to the emergence of two isolated hydrogen atoms of order $2\varepsilon_{des}(1H)$ (Fig. 12). The subsequent recombination results in a decrease in the system energy.

The second trajectory (Fig. 11b) is optimized for the energetics of H atoms leaving the surface. The atoms initially approach each other along the surface to an interatomic distance of d_{min}, passing from positions above opposite edges of the tungsten cell to positions above the nearest edges of a single surface tungsten cell. In the case of such trajectory, the system energy increases monotonically. The desorption activation energy in this case is ε_{des} (H_2) ≈ 1.85 eV. Thus, for the desorption process of a pair of H atoms separated by distances greater than d_{min}, it is energetically favorable for them to initially approach along the surface to a minimum distance of d_{min}. For such a pair of adsorbed H atoms, there is a vertical synchronous (correlated) emergence of two atoms from the layer with a high electron density of metal atoms.

3.7. Recombinative desorption from clusters

Hydrogen release from clusters depends on the size and configuration of the clusters. Fig. 13a shows the release of two hydrogen atoms from a linear cluster of four atoms with an interatomic distance of d_{min}. The calculated activation energy for this process is $\varepsilon_{des} \approx 1.56$ eV. Fig. 13b shows the release of a pair of H atoms into vacuum from a dense cluster of 12 atoms with an interatomic distance of about d_{min} and a local coverage θ = 2. The calculated activation energy for this process is $\varepsilon_{des} \approx 1.31$ eV.

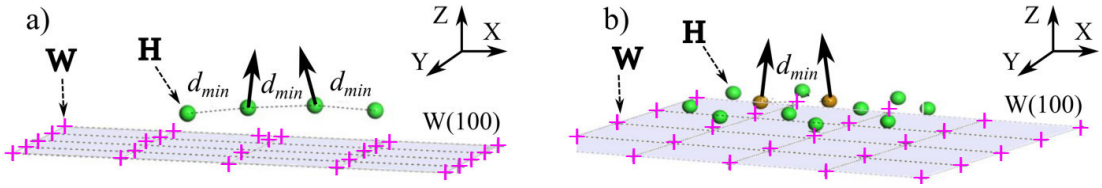

Fig. 13. Desorption of two H atoms from clusters with different numbers of atoms H: a – desorption from a linear cluster of four atoms with interatomic distance d_{min}- desorption from the internal region of a dense cluster of 12 atoms with interatomic distance d_{min}. All W atoms are shown by crosses

Thus, the presence of adsorbed hydrogen atoms on the surface, adjacent to the recombining pair of H atoms, reduces the activation energy for molecule desorption H_2 to values $\varepsilon_{des} \approx 1.56$ and 1.31 eV (in the absence of neighbors ε_{des} (H_2) ≈ 1.85 eV). The high density of hydrogen atoms in clusters on the surface leads to an increase in their interaction along the surface and a decrease in the activation energy for hydrogen release into vacuum. This result corresponds to the fact that recombination becomes a many-body process rather than the second order one.

3.8. Desorption involving subsurface hydrogen atoms

This section examines the influence of hydrogen atoms "floating up" from the tungsten bulk on the processes of recombinative desorption.

Fig. 14 shows the configuration of a cluster of nine atoms with interatomic distance $d = 3.15$ Å (local coverage degree $\theta = 1$). Absorbed clustered H atoms are located in the bridge positions over the upper layer of W atoms. The free H atom is located initially in a tetrapore below the surface. This atom can penetrate without barrier into the layer of adsorbed hydrogen atoms of the cluster and occupy the site between four initially absorbed atoms (side view and top view are shown). The distance between the "floated up" H atom and the nearest adsorbed atom of the upper layer is d(H–H) $\approx$ 1.8-2.0 Å. From this state, a recombinative desorption process of an atom pair is possible (H atom emerged from the bulk under the cluster and a cluster atom). The activation energy for desorption of this pair is $\varepsilon_{des} \approx 1.56$ eV.

Fig. 15 shows the configuration of a dense cluster of 16 atoms with the local coverage $\theta = 2$ (interatomic distance about d_{min}) and an H atom that emerges from the tungsten bulk under this cluster into the space between the cluster and surface W atoms. Unlike Fig. 14, all states above the W surface in this case are occupied. Calculations show that the inner cluster atom can combine with the floating up atom, and the activation energy of recombinative desorption in this case equals $\varepsilon_{des} \approx 1.0$ eV.

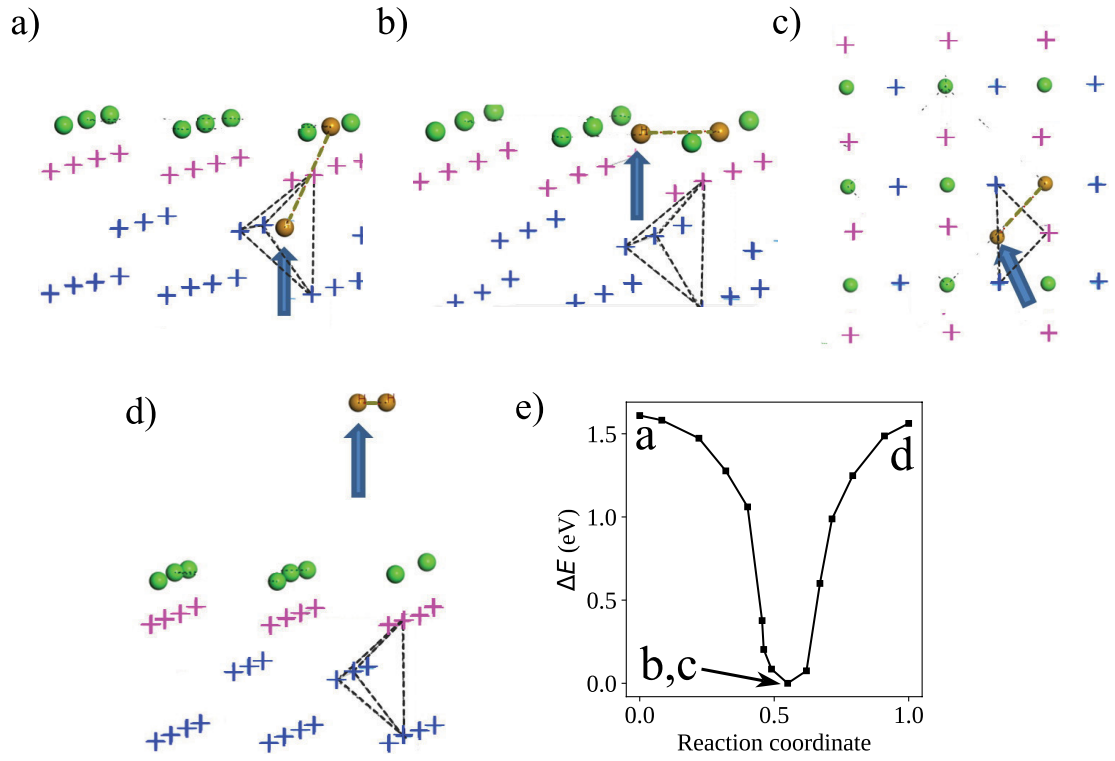

Fig. 14. "Surfacing" and recombinative desorption of an H atom that emerges from the W tetrapore under a cluster of nine H atoms; blue arrows indicate this atom, and red spheres highlight the pair of H atoms leaving the surface. All W atoms are shown as crosses: a) – near-surface interstitial H atom is located in a tetrapore; b) and c) represent H atom transitions into the layer of adsorbed hydrogen atoms in the position between four adsorbed atoms (b) – side view, c) – top view); d) shows possible process of desorption of an atom pair as a molecule H_2 involving the "surfaced" H atom and a boundary cluster atom; e) a change in the system energy during the movements shown in Fig. 14a-d: the reference level for coordinates and energy corresponds to Fig. 14b, c

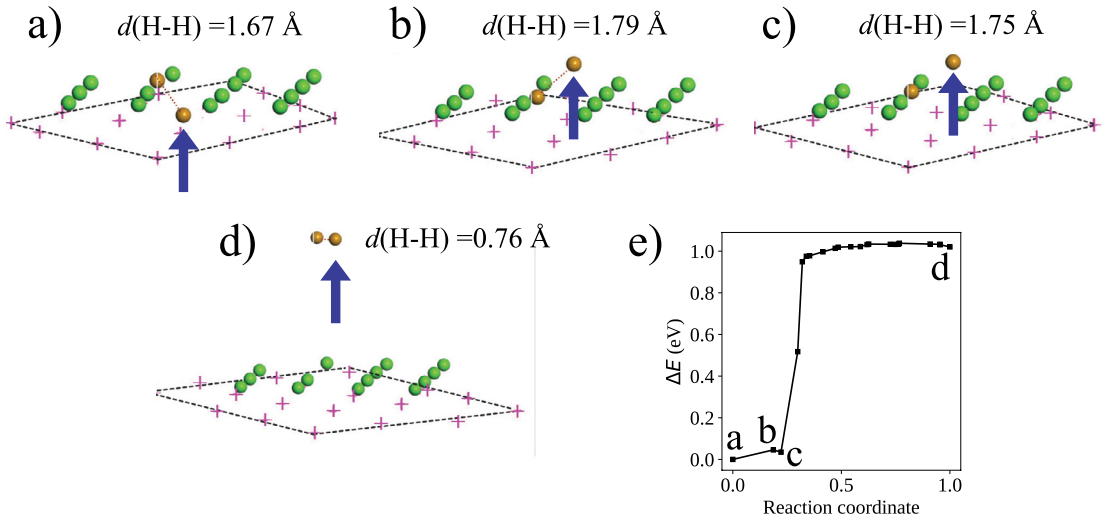

Fig. 15. Recombinative desorption of an H atom that emerged from the W bulk under a cluster of 16 H atoms with the interatomic distance d_{min} (local coverage degree $\theta = 2$); arrows and red spheres highlight the pair of H atoms leaving the surface. The H atom that emerges from the bulk is indicated by a thick blue arrow. All W atoms are shown as crosses: *a* – near-surface interstitial H atom that emerged from the W bulk under the cluster (local coverage degree $\theta = 2$); *b, c, d* represent stages of the desorption process of an atom pair as a molecule H_2; *e* is a change in the system energy during the movements shown in Fig. 15a-d; the reference level is taken as the energy of the system configuration corresponding to Fig. 15a

It should be noted that another recombination process, in which the floating up atom displaces the nearest atom of the inner region upward above the cluster, while taking the place of the latter in the cluster plane. The activation energy for subsequent desorption of the resulting pair is also $\varepsilon_{des} \approx 1.0$ eV.

3.9. Critical size for desorption from a dense cluster

After transition of an H atom from the near-surface layers of tungsten under a small dense cluster of hydrogen atoms adsorbed on the surface, three processes are possible: growth of the cluster, formation of a second intermediate layer of hydrogen atoms, and recombinative desorption. If the cluster size is small, its growth is more likely; otherwise, the formation of a second layer and desorption by the mechanism considered above are possible. Let us consider the question of the smallest size of a dense cluster, at which the desorption process is still possible.

Fig. 16 shows the initial optimized configuration after the “surfacing” of an H atom under the central region of a dense cluster of six adsorbed atoms with an interatomic distance of $d(\mathrm{H-H}) \approx 2.3$ Å. The central atom of this cluster is surrounded by other atoms on all sides. This is the minimal configuration with such surrounding of this

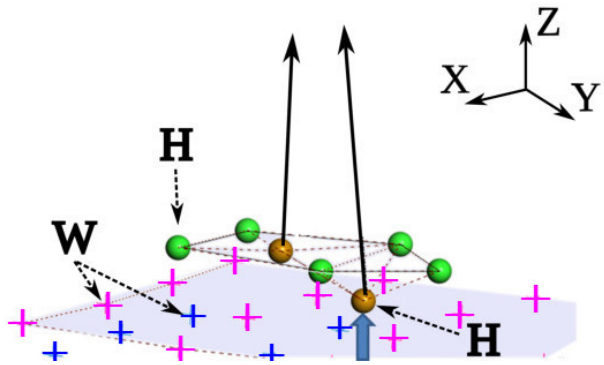

Fig. 16. Optimized configuration after “surfacing” of an H atom under the dense cluster of six adsorbed atoms with interatomic distance $d(\mathrm{H-H}) \approx 2.3$ Å, for which the central atom of this cluster is surrounded by other atoms from all sides (the tungsten surface plane is highlighted in gray). Arrows and red spheres highlight the pair of H atoms leaving the surface. The H atom that came from the array is shown with a thick blue arrow

H atom. The activation energy for recombination and desorption of the central atom of the cluster containing six hydrogen atoms and the “surfaced” H atom from the bulk equals 0.97 eV.

The minimum activation energy for recombinative desorption of an H atom "floating up" from the bulk and an innner H atom from a cluster of about 6 atoms is $\varepsilon_{des} \approx 0.94$ eV. Similar processes can take place also in the cases of dense clusters containing more than six atoms. Clusters containing about six hydrogen atoms can be considered critical.

4. CONCLUSION

In this work, the following has been shown through *ab initio* modeling.

1. Energy barriers for approach of two distant on-surface hydrogen atoms (approximately 0.6 eV) and between a single atom and a cluster of adsorbed hydrogen atoms (~ 1.0 eV) are somewhat higher than the activation energy for surface diffusion of single hydrogen atoms $\varepsilon_{dif} \approx 0.22$–$0.43$ eV [3, 29, 41, 42]. Thus, the movement of atoms along the surface W(100) is not an effective mechanism for the growth of adsorbed hydrogen atom clusters.

2. Hydrogen atoms that have diffused into the under-surface of tungsten from its bulk are adsorbed on the surface without activation if the surface coverage is low. This can facilitate cluster growth on the surface and recombinative desorption.

3. The "surfacing" of hydrogen atoms from the tungsten bulk to its subsurface can lead to the growth of existing surface clusters or increase their local density in their internal zones. Two growth mechanisms are possible: hydrogen atom adsorption at the cluster boundary if H atom appears near it, and displacement of one inner atom of the cluster to the periphery if the hydrogen atom appears in the middle of the cluster. The first process is possible for clusters of any size, the second process is shown for clusters with sizes not exceeding six atoms. The energy barrier for cluster decomposition is about 0.6 eV, which exceeds the activation energy for diffusion of single adsorbed atoms.

4. For the process of recombinative desorption of hydrogen from the surface, the principal factors are the interatomic distance in the recombining pair and the local environment of this pair of atoms, rather than just the average surface coverage by adsorbed H atoms. The activation energy for desorption of an isolated pair of hydrogen atoms located at adjacent equilibrium sites (with interatomic distance $d(\mathrm{H}-\mathrm{H}) \approx 2.3$ Å) equals $\varepsilon_{des} \approx 1.85$ eV. If there are some other H atoms located in the neighbour sites to the recombining pair, the activation energy for molecular desorption H_2 decreases to values less than $\varepsilon_{des} \approx 1.5$ eV depending on the local environment.

5. For the atomically smooth W(100) surface, the recombinative desorption of an adsorbed H atom from a dense cluster of the first layer from the bulk and an H atom that has emerged under this layer from this bulk has the lowest desorption activation energy $\varepsilon_{des} \approx 0.9$-$1.0$ eV, which is due to the small interatomic distance. The activation energy from the atomically smooth surface W(100) is close to the activation energy values typical for experiments on thermal desorption after ion implantation, where the rate-limiting step is usually suggested to be hydrogen release from vacancy-type traps in the tungsten bulk (about 1.0–1.4 eV) [7, 35, 43–46]. The probability of other recombination desorption channels from the atomically smooth W(100) surface is lower. Further, we will also consider the influence of surface defects on W(100) on the recombinative desorption process.

The calculation results in this work are presented without taking into account zero-point vibrations of hydrogen atoms; estimates of the contribution of this effect based on the calculated vibrational spectra of hydrogen atoms on the surface for certain configurations give values of about tenths of eV/(H atom), which may be important for hydrogen diffusion processes but has little effect on desorption barriers. Comparative analysis based on Gibbs thermodynamic potential was not attemped as such calculations considering configurational interaction is an independent task that requires analysis of all possible coverage degrees for multiple configurations, including spatially inhomogeneous ones, taking into account the phonon contribution to entropy for each configuration. Attempts at such calculations were made in work [47] for uniform coverage of adsorbed hydrogen and for a relatively small cell size (2×2 elementary cells), modeling the tungsten surface, which does not allow describing the possibility of dense hydrogen atom clusters on the surface. In this work, we limited ourselves to a comparative analysis of energy barriers for a series of probable processes without considering thermal effects.

FUNDING

This work was supported by the Ministry of Science and Higher Education of the Russian Federation (grant No. 0723-2020-0043).

REFERENCES

1. G. Pintsuk, in:Comprehensive Nuclear Materials, ed. by R. J. M. Konings, Elsevier, Vol. 4 (2012), p. 551.

2. R. A. Pitts, X. Bonnin, F. Escourbiac et al., Nucl. Mater. Energy 20, 100696 (2019).

3. D. F. Johnson and E. A. Carter, J. Mat. Research 25, 315 (2010).

4. M. Yajima, Y. Hatano, N. Ohno et al., Nucl. Mater. Energy 21, 100699 (2019).

5. V. N. Fateev, O. K. Alekseyeva, S. V. Korobtsev et al., Chemical Problems 16, 453 (2018).

6. J. Roth and K. Schmid, Phys. Scr. 145, 014031 (2011).

7. X.-S. Kong, S. Wang, X. Wu et al., Acta Materialia 84, 426 (2015).

8. J. Guterl, R. D. Smirnov, S. I. Krasheninnikov et. al., J. Nucl. Mater. 463, 263 (2015).

9. V. Kulagin, Y. Gasparyan, and N. Degtyarenko, Fusion Engineering and Design 184, 113287 (2022).

10. M. W. Finnis and J. E. Sinclair, Phil. Mag. A 50, 45 (1984).

11. B. J. Lee, M. I. Baskes, H. Kim et al., Phys. Rev. B 64, 184102 (2001).

12. P. M. Derlet, D. Nguyen-Manh, and S. L. Dudarev, Phys. Rev. B 76, 054107 (2007).

13. M. Mrovec, R. Groger, A. G. Bailey et al., Phys. Rev. B 75, 104119 (2007)..

14. X. C. Li, X. Shu, Y. N. Liu et al., J. Nucl. Mater. 408, 12 (2011)..

15. G. Y. Pan, Y. G. Li, Y. S. Zhang et al., RSC Adv. 7, 25789 (2017).

16. T. E. Felter, R. A. Barker, and P. J. Estrup, Phys. Rev. Lett. 38, 1138 (1977).

17. M. K. Debe and D. A. King, Phys. Rev. Lett. 39, 708 (1977).

18. M. S. Altman, P. J. Estrup, and I. K. Robinson, Phys. Rev. B 38, 5211 (1988).

19. R. Yu, H. Krakauer, and D. Singh, Phys. Rev. B 45, 8671 (1992).

20. W. Xu and J. B. Adams, Surf. Sci. 319, 45 (1994).

21. H. F. Busnengo and A. E. Martinez, Phys. Chem. C 112, 5579 (2008).

22. L. Sun, Y.-N. Liu, W. Xiao et al., Materials Today Communications 17, 511 (2018).

23. D. A. King and G. Thomas, Surf. Sci. 92, 201 (1980).

24. A. Adnot and J. D. Carette, Phys. Rev. Lett. 39, 209 (1977).

25. M. R. Barnes and R. F. Willis, Phys. Rev. Lett. 41, 1729 (1978).

26. K. O. E. Henriksson, K. Nordlund, A. Krasheninnikov et. al, Fusion Sci. Technol. 50, 43 (2006).

27. C. Becquart and C. Domain, J. Nucl. Mater. 386388, 109 (2009).

28. P. Alnot, A. Cassuto, and D. A. King, Surf. Sci. 215, 29 (1989).

29. K. Heinola and T. Ahlgren, Phys. Rev. B 81, 073409 (2010).

30. A. Moitra and K. Solanki, Computational Materials Science 50, 2291 (2011).

31. Z. A. Piazza, M. Ajmalghan, Y. Ferro, and R.D. Kolasinski, Acta Materialia 145, 388 (2018).

32. R. A. Barker and P. J. Estrup, J. Chem. Phys. 74, 1442 (1981).

33. L. Cai, M. S. Altman, E. Granato et al., Phys. Rev. Lett. 88, 226105 (2002).

34. G. Pan, Y. Zhang, Y. Li et al., International Journal of Modern Physics C 28, 1750090 (2017).

35. E. Hodille, M. Payet, V. Marascu et. al., Nucl. Fusion 61, 086030 (2021).

36. Y. Ferro, E. A. Hodille, J. Denis et al., Nucl. Fusion 63, 036017 (2023).

37. M. Ajmalghan, Z. A. Piazza, E. A. Hodille et al., Nucl. Fusion 59, 106022 (2019).

38. T. W. Hickmott, J. Chem. Phys. 32, 810 (1960).

39. P. Giannozzi, S. Baroni, N. Bonini et al., J. Phys.: Condens. Matter 21, 395502 (2009).

40. P. Giannozzi, O. Andreussi, T. Brumme, et al., J. Phys.: Condens. Matter 29, 465901 (2017).

41. N. N. Degtyarenko and A A Pisarev, Physics Procedia 71, 30 (2015).

42. N. N. Degtyarenko and A A Pisarev, J. Phys.: Conference Series 748, 012010 (2018).

43. K. Nordlund, J. Keinonen, Phys. Rev. B 82, 094102 (2010).

44. E. Hodille, X. Bonnin, R. Bisson et al., J. Nucl. Mater 467, 424 (2015).

45. E A Hodille, Y Ferro, N Fernandez et al., Physica Scripta T167, 014011 (2016).

46. K. Heinola, T. Ahlgren, K. Nordlund et al., Phys. Rev. B 82, 094102 (2010).

47. Z. Piazza, R. Kolasinski, M. Ajmalghan, E. Hodille, Y. Ferro, J. Phys. Chem. C 125, 16086 (2021).